**Journal of Physical and Theoretical Chemistry**
of Islamic Azad University of Iran , 6 (1) 1 - 7: Spring 2009
(J.Phys.Theor.Chem.IAU Iran)
ISSN: 1735-2126

# Synthesis and Ethanol Sensitivities of $SnO_2$ nanowires Suvit

Thanasanvorakun[1], Pongsri Mangkorntong[1], Majid Monajjemi[2,*] and Nikorn Sangkorntong[1]

[1] Department of Physics, Faculty of Science, Chiang Mai University, Chiang Mai 50200, Thailand
[2] Departments of Chemistry, Science and Research Branch, Islamic Azad University, Tehran, Iran

## ABSTRACT

$SnO_2$ nanowires with diameters of 30 – 200 nm have been synthesized by using carbothermal process via a thick film of tin dioxide and carbon powder precursor. The nanowires were characterized by X-ray power diffraction (XRD), scanning electron microscopy (SEM), transmission electron microscopy (TEM) and Selected Area Electron Diffraction (SAED). The gas sensing characteristic of nanowires toward ethanol vapor was investigated. The gas sensitivity experiments have demonstrated that the as-synthesized $SnO_2$ materials exhibit good sensitivity to ethanol vapors, which may offer potential applications in gas sensors. The details of its sensing characteristics were observed and discussed.

**Keywords:** carbothermal; nanowires; resistivity; rutile.

## INTRODUCTION

Metal oxide has attracted considerable attention for a long time for their gas sensing property due to their advantageous features, such as higher sensitivity to ambient conditions, lower cost, and simplicity in fabrication. Among these semiconductors, the rutile form of $SnO_2$ is one of the interesting materials. It is an n-type semiconductor with a wide band gap of 3.6 eV at room temperature, and is well known for its applications in gas sensors [1], capacitors [2], transistors [3], and solar cells [4]. So far, considerable effort has been devoted to the synthesis of nanostructured $SnO_2$ materials, including nanoparticles, nanowires, nanorods, and nanobelts [5–8]. At above 200 $^0$C, the adsorption of negatively charged oxygen will produce a potential barrier to establish a resistive electron depletion layer near the surface of n-type oxide semiconductor. The interaction between oxidation/reduction gases and oxygen ion species will create a large enough change in the electrical conductivity allowing it to be employed in gas sensor application. Recently, it has been reported that $SnO_2$ nanowires are promising for gas sensors due to the high surface-to-volume ratio, high purity due to its the single crystalline structure and consistent size which results in easy to produce a complete depletion of carriers inside the wire [8]. Therefore, the tin oxide nanowires have been widely employed as sensors for ethanol, CO and other gases, mostly in the bulk form [9-10]. So far single wire form has been reported only for carbon monoxide sensor, but not ethanol sensor [11].

*.Corresponding author : M. Monajjemi

# EXPERIMENTAL

## Synthesized

$SnO_2$ nanowires were prepared by carbothermal process. All commercially starting materials, tin dioxide ($SnO_2$) and carbon (C) powders were mixed in a ratio of 1:5 (w/w) and then were hand-grounded in an agate mortar with polyvinyl alcohol (PVA). After that, the mixture was screened onto the alumina substrate and placed in an alumina boat with copper oxide powder laid underneath the substrate. The boat was then rapidly heated in a horizontal tube furnace which had been kept at the temperature of 800 $^0$C, for 1 hr. in normal atmospheric pressure, without any inert gas.

## Characterization

After cooling down to room temperature, some white wool-like scattered thoroughly on the substrate surface were observed. A Seamens-D500 diffractometer with Cu $K_\alpha$ radiation at 40 kV ($\lambda$ = 0.1542 nm) were employed for identifying the synthesized products. The sample was scanned for a 2$\theta$ from $10^0$ to $60^0$ in a step of $0.16^0$. Lattice parameters of these products were determined from XRD pattern. The morphologies and sizes of the products were characterized by scanning electron microscopy (SEM), FEI Quanta 3D (200) operated at 30 kV. To obtain more information, transmission electron microscopy (TEM) and the typical selected area electron diffraction (SAED) pattern have been taken on JEOL JEM-2010 operated at 200 kV.

## Gas sensor measurements

Gas sensors were fabricated by coated Au interdigital electrode over an assembly of the $SnO_2$ nanowires. Then, they were calcined at 500 $^0$C for 2 h in air. The operating temperature of the sensors was varied from 200 to 320 $^0$C. The sensitivity (S) of the sensors was defined as ($R_a/R_g$), where $R_a$ and $R_g$ are the resistances in air and the gas, respectively. The gas sensing characteristics of the sensor were investigated by recording online the electrical response of the sensor to periodical changes between air and saturated vapors of ethanol using a home-made electric circuit at room temperature. The electrical voltage of the sensor was measured by a Kiethley digital multimeter model 196 and collected by input into a computer. The saturated gas vapors were obtained in a bottle containing the liquids of the ethanol where gas–liquid equilibrium was regarded to be achieved after standing for a long time.

# RESULTS AND DISCUSSION

## Characterize

There were 8 peaks with 2$\theta$ values of 26.48, 33.87, 37.91, 38.98, 51.72, 54.85, and 57.97 have collected by the X-ray diffraction (XRD) pattern (Fig. 1). All of diffraction peaks corresponding to $SnO_2$ crystal planes of (110), (101), (200), (111), (211), (220), and (002), respectively. These diffraction peaks can be indexed to the tetragonal rutile structure of $SnO_2$ with lattice constants a = b = 4.734 Å and c = 3.185 Å, respectively, which are consistent with the standard values of bulk $SnO_2$ (JCPDS 880287). Thus, the XRD result implies that the as-synthesized products were pure rutile $SnO_2$.

Fig. 2 illustrates the images from the scanning electron microscope (SEM). It revealed that their geometrical structure were wire and rod-liked. In the wire-like structure, their widths were 10 – 120 nm with the typical size of about 30 nm and their length were estimated up to several hundred micrometers. Furthermore, fig. 2c show bending nanowire that has a function of high flexibility. In addition to the wire-shape, belts-likes nanowires were also observed. Typical widths and thickness of the belts-likes nanowires were in the range of 30 – 200 nm and 10–30 nm, respectively.

Transmission electron microscope (TEM) and area diffraction (SAED) were utilized to demonstrate the detailed structure of the $SnO_2$ nanowires. Fig.3a shows a TEM bright field image of a selected nanowire which revealed

that it was a single crystalline without any dislocation. The inset SAED pattern of the nanowires in Fig.3b was recorded with the electron beam along [020] .

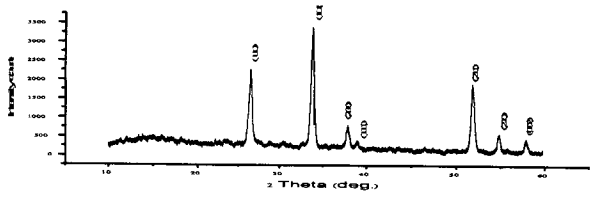


**Fig. 1.** A typical XRD pattern of the $SnO_2$ nanowires obtained from Cu Kα radiation.

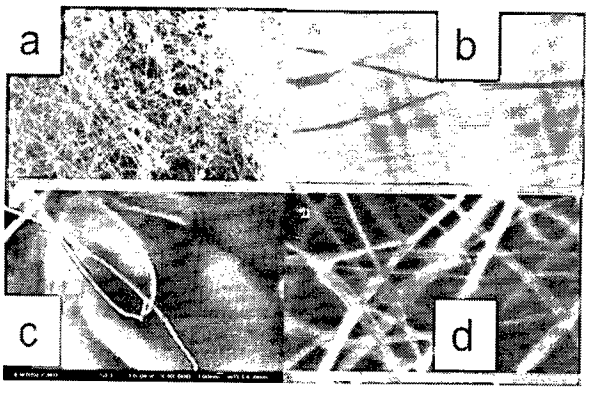


**Fig. 2.** SEM images: **(a)** a group of nanowires, **(b)** Y-shape of nanowires **(c)** bending nanowire and **(d)** nanowire with a tip growth.

From the SAED, the growth direction of $SnO_2$ nanowire was found to be [101], in agreement with previous reports [12, 13]. The TEM observations showed that the growth behavior of the $SnO_2$ nanowires might not be dominated by the vapor–liquid–solid process proposed for a one dimensional nanostructure, in which a catalytic metal particle was located at the growth front and acts as the energetically favorable site [13].

Since a significant feature of the VLS mechanism was, there were no catalytic droplets observed on neither end of the nanowires. Consequently, we can hypothesize that the $SnO_2$ nanowires, in this work, prefer undergo a vapor-solid growth process.

Rutile $SnO_2$ belong to the point group $D_{4h}^{14}$ and space group $P4_n/mnm$, of which the normal lattice vibration at the Γ point of the brillouin zone is given on basis of group theory

$$\Gamma = A_{1g} + A_{2g} + B_{1g} + B_{2g} + E_g + 2A_{2u} + 2B_{1u} + 4E_u$$

Among them, the active Raman modes are $B_{1g}$, $E_g$, $A_{1g}$, and $B_{2g}$, and consequently four first-order Raman spectra are observed. In the Raman active modes the oxygen atoms vibrate while the Sn atoms are at rest. The modes of $A_{1g}$ and $B_{2g}$ vibrate in the plane perpendicular to the c-axis while the $E_g$ mode vibrates in the direction of the c-axis [14].

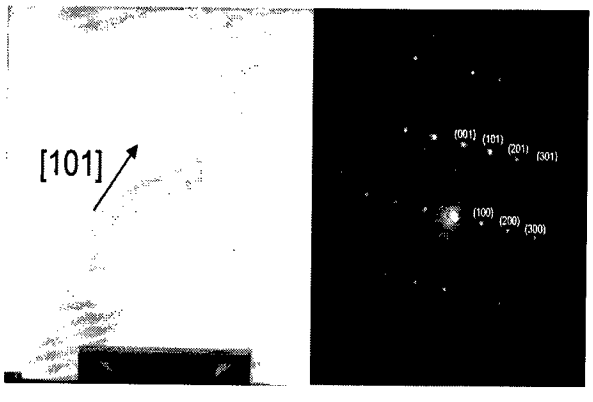


**Fig. 3. (a)** TEM image of an individual nanowire, **(b)** SAED pattern taken along [0 2 0].

The Raman peaks of the starting $SnO_2$ powder were detected at 474.7, 634.6, and 776.6 $cm^{-1}$, corresponding to the $E_g$, $A_{1g}$, and $B_{2g}$ vibration modes of rutile bulk $SnO_2$, respectively. While the Raman peaks of the $SnO_2$ nanowires appeared at 475.0, 634.6, and 772.5 $cm^{-1}$. Thus, these peaks provide confirmation that $SnO_2$ nanowires possess the crystalline structure of the tetragonal rutile structure similar to that of the powder. In the Raman spectrum of the $SnO_2$ nanowires, the mode $A_{1g}$ and $B_{2g}$ shift toward lower wave numbers while the mode $E_g$ shifts toward higher wave numbers. A small dimension of the nanowires leads to a downshift of the Raman peaks, while stress trends to shift Raman peak to a higher frequency region [14].

There are at least two models that can be proposed to describe the growth mechanism of the one-dimensional materials, such as VLS (vapor–liquid–solid) and VS (vapor–

solid) mechanisms. It was proposed that a way to verify the mechanisms is the present of a tip growth. The SEM in this work reveals that both mechanisms are possible. Fig.2 (d) illustrate a tip growth which represents VLS mechanism, although not much but it is likely that the growth of $SnO_2$ nanowires is dominated by the vapor–solid (VS) mechanism [13].

Since the results were confirmed that $SnO_2$ nanowires performed single crystal. There are 2 conditions concerned nanostructure and single crystal. One is single crystal basically grow from vapor and the other one is influence by the content of $O_2$, therefore this would have an effect on its size. A carbothermal reduction is typically an approach to the synthesis of a wide range of nanostructure metal oxides. However, it is unclear how the role of carbon will be employed to produce nanostructure. Let us consider the enthalpy between the following reactions,

$$C(s) + O_2 \longrightarrow CO_2(g) \quad : \Delta H = -393.3 \text{ kcal/mol}$$

$$SnO(g) + \tfrac{1}{2} O_2(g) \longrightarrow SnO_2(s) \quad : \Delta H = -134.9 \text{ kcal/mol}$$

One can see that $O_2$ favors the reaction with C rather than SnO. This suggests that the carbon and oxygen reaction will decrease the amount of $O_2$ in the system so the required condition of nanostructure would be supported. To construct $SnO_2$ the source vapor constructing $SnO_2$ nanowires should be supplied from the source materials. Hence, the source materials could be Sn (g) + $O_2$, SnO (g) + $O_2$ or $SnO_2$ (g) depending on the process. In this work, $SnO_2$ powder was firstly reduced by active carbon powder at 700 $^0$C yield SnO and CO, described in (1).

$$C(s) + SnO_2(s) \longrightarrow SnO(g) + CO(g) \qquad (1)$$

Normally, the phase transformation from SnO to $SnO_2$ in an ambient atmosphere may be occurred as low as 370 $^0$C but usually in the powder form not the nano form if heated alone. Then $SnO_2$ powder will continue to be reduced by the CO gas formed from reaction (1).

$$CO(g) + SnO_2(s) \longrightarrow SnO(g) + CO_2(g) \qquad (2)$$

SnO vapor is the common resultant of these two reactions, shown above.

As we all know SnO is metastable, it will decompose into Sn and $SnO_2$ above 600 $^o$C, as shown in reaction (3). Considering the low melting point of Tin (231.9 $^o$C), Sn particles are still liquid at reaction temperature. These Sn droplets fell on the substrate and can provide the energetically favored sites for adsorption of $SnO_2$ vapor. Subsequently, the decomposition of SnO will result in the precipitation of $SnO_2$ and the $SnO_2$ nanowires are formed.

$$SnO(g) \longrightarrow Sn(l) + SnO_2(g) \qquad (3)$$

**Ethanol Sensing**

It is well known that metal oxide-based gas sensors changes their conductivity in the presence of a gas. Typically, in vacuum metal oxide exhibit as a conductor but in the normal atmosphere it acts like semiconductor. This effect is believed that adsorbed oxygen ions ($O^-$, $O^{2-}$ and $O_2^-$) have a dominant role in the response of metal oxide to a reducing/oxidizing gas. Sensing mechanism can be described as oxygen when it is first adsorbed on any surface (including the metal oxide surface) at room temperature in normal atmosphere. Since metal oxides were heated to the operating temperature, higher than 150 $^o$C, the absorbed oxygen can be interacted with electrons at the surface via thermal energy. In the case of an n-type semiconductor such as $SnO_2$, the electrons are drawn from ionized donors via the conduction band. So the charge electrons density at the crystal surface is transferred to the adsorbed oxygen, resulting in an increase in resistivity. Thus, surface potential is formed to serve as a potential barrier against electron flow as shown in Fig. 5. There are three possible species of charged oxygen detected on metal oxide surface in an oxidizing environment. The chemical reaction between oxygen and electron can be described as following reactions:

$$O_2 + e^- \longrightarrow O_2^-$$

$$O + e^- \longrightarrow O^-$$

Or

$$O + 2e^- \longrightarrow O^{2-}$$

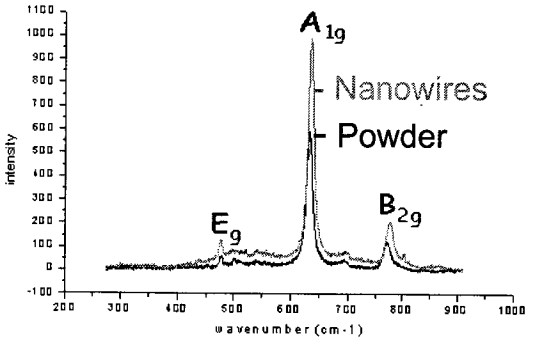


**Fig. 4.** Comparison of Raman pectrum.

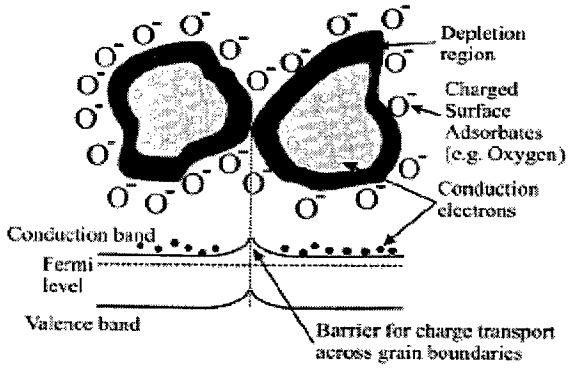


**Fig. 5.** Model of charge carrier concentration in $SnO_2$ grains.

The different oxygen ion species adsorption depends on temperature for example $O^-$ and $O^{2-}$ reaction will occur at temperature higher than 150 °C. Whereas, $O_2^-$ reaction will take place at any temperature lower than 150 °C, as shown by EPR (Electron Paramagnetic Resonance) results [15]. In the presence of reducing gas these oxygen ion species will be deprived. Consider a simple reducing gas like $H_2$ or CO, which deprives the oxide surface of one $O^-$ ion per molecule, as describe in the following reaction.

$$A + O^-_{surf} \longrightarrow AO + e^-$$

Electron from this reaction will create changes in the resistivity. Thus, when a reaction take place between metal oxide and reducing gas, one should observed the changing in electivity. So in the presence of a reactive gas the surface density of the negatively charged oxygen may decrease as a consequence of the reduction in the resistance.

The mechanism of ethanol sensing is complex and not yet completely established. Jinkawa et al. [16] reported that the decomposition of ethanol at elevated temperatures depended on the acid–base properties of the oxide catalyst used.

$$C_2H_5OH(g) \rightarrow CH_3CHO(g) + H_2(g)$$

(basic oxide) (1)

$$C_2H_5OH(g) \rightarrow C_2H_4(g) + H_2O(g)$$

(acidic oxide) (2)

It was suggested that the higher gas response of the basic-oxide reaction shows that the oxidation of $CH_3CHO+H_2$ with the negatively charged surface oxygen ( $O^-_{surf}$) induces a larger increase in conductance than that of $C_2H_4$ , as shown below.

$$C_2H_5OH + O^-_{surf} \rightarrow \quad CH_3CHO + H_2O + e^-$$

Since $SnO_2$ exposure with ethanol vapor at operating temperature, one can expected a decrease in electrical resistance.

Gas sensor characterization usually requires two kinds of measurements:

• determination of the temperature at which the sensor reaches the maximum sensitivity to a given gas at the constant concentration.

$$S = \frac{R_a}{R_g}$$

here $R_a$ is the electrical resistance of sensor in air and $R_g$ is the electrical resistance of sensor in ethanol-air mixed gas.

• time response are measured for the sensor operating at the constant temperature and gas concentration,

$$\tau^-_{90} = T_g - T_a$$

In this work, the sensing curves of ethanol sensors were detected under an ethanol vapor at various concentration 100 - 1000 ppm and operating temperatures between 200-320°C as shown in fig. 6. As describe above, oxygen ions species ($O^-$, $O^{2-}$ and $O_2^-$) have a

dominant role in the response of metal oxide and this evidence cause an increasing in resistivity. However, at operating temperature thermal energy is high enough to shift electron from valence band to conduction band. Hence, the decreased in electrical resistance was normally observed when the operating temperature increased. Explicitly, the characteristics of sensor depend on the operating temperatures. Fig.3a, shown ethanol sensing characteristic of the sensor at concentration of 100 ppm in various operating temperatures. It was found that, at operating temperature of about 280°C presented the highest sensitivity of the sensors in every concentration. The response to 100, 500 and 1000 ppm ethanol was 26, 48 and 54, respectively, which increased approximately linearly with increasing ethanol concentration. In order to screen intoxicated drivers, the ethanol sensor should be able to detect [$C_2H_5OH$] > 200 ppm, which corresponds > 0.5 g of $C_2H_5OH$ per liter of blood [17, 18].

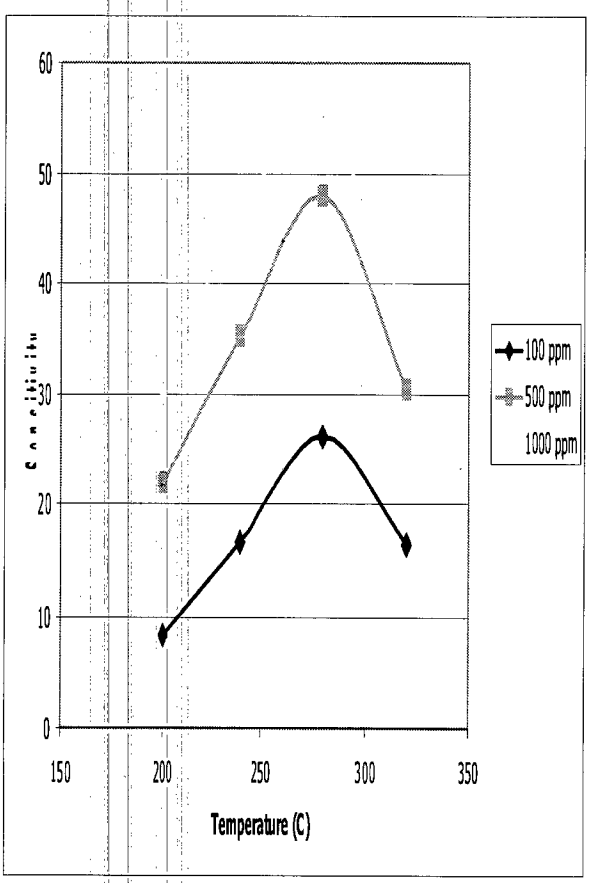


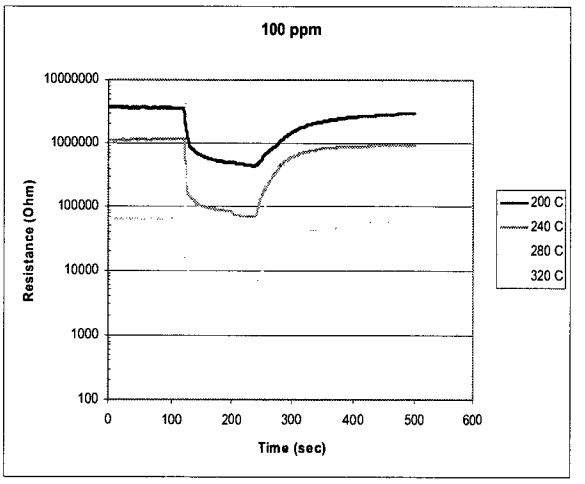


**Fig.6. a)** Sensing characteristics of sensors under an ethanol vapor at concentration of 100 ppm in various operating temperatures **b)** Sensitivity characteristics of sensors in different concentration.

The response time ($\tau^-_{90}$) and also recovery time ($\tau^+_{90}$) as a function of operating temperature of 200-320°C of sensors was plotted in fig.7 (a) and (b), respectively. The plot showed that the recovery time decreased with increasing operating temperatures.

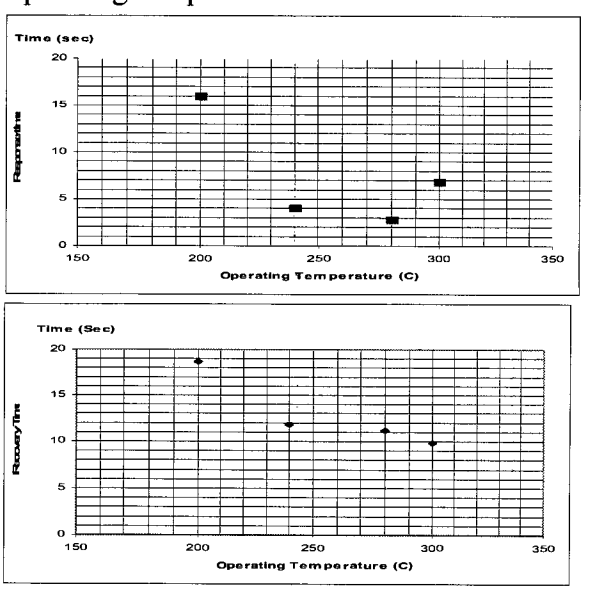


**Fig.7.** Plot of response time ($\tau^-_{90}$) and recovery time ($\tau^+_{90}$) of the sensors under ethanol vapor at concentration of 100 ppm and at various operating temperatures of 200-320°C.

## CONCLUSION

The carbothermal reduction process was employed to synthesis $SnO_2$ nanowires. Since The experimental results implied that these nanowires were single crystalline with pure fabrication of nanostructure required the optimum amount of $O_2$ thus the carbon and oxygen reaction will support as diminution the amount of $O_2$ in the system.

Rutile $SnO_2$ which undergoes Vapour-Solid growth process. The sensor performed highest sensitivity at operating temperature about 280 °C for every ethanol vapor concentration. It was found that response time and recovery time are In the future, it is possible for $SnO_2$ nanowires to be utilize for gas sensing application as the the function of operating temperature.

Moreover, the recovery time decreased With increasing operating temperatures.findings illustrate that it exhibit good sensitivity to ethanol vapour.

## ACKNOWLEDGEMENT

We would like to thank the Nanoscience and Nanotechnology Center Project, Faculty of Science, Chiang Mai University and the Network for Excellence in Functional Nanomaterials, Chiang Mai University for their support. NANOTEC, Thailand is also acknowledged. Suvit Thanasanvorakun would like to acknowledge the Graduate School, Chiang Mai University for financial support.

## REFERENCES

[1] S.G. Anasari, P. Boroojerdian, S.R. Sainkar, R.N. Karekar, R.C. Aiyer and S.K. Kulkarni, *Thin Solid Films* 295 **(1997)** 271.

[2] K.R. Prasad and N. Miura, *Electrochem. Commun.* 6**(2004)** 849.

[3] G. Sberveglieri, *Sens. Actuator B* 6 **(1992)** 239.

[4] M. Turrion, J. Bisquert and P. Salvador, *J. Phys. Chem. B* 107 **(2003)** 9397.

[5] Kolmakov, Y. Zhang, G. Cheng and M. Moskovits, *Adv. Mater.* 15 **(2003)** 997.

[6] X.L. Ma, Y. Li and Y.L. Zhu, *Chem. Phys. Lett.* 376 **(2003)** 794.

[7] S. Thanasanvorakun, P. Mangkorntong, S. Choopun and N. Mangkorntong, *Ceramics International*

[8] E. Comini, G. Faglia, G. Sbervegleiri, Z.W. Wei and Z.L. Wang, *Appl. Phys. Lett.* 82 **(2002)** 286.

[9] E. Comini, G. Faglia, G. Sberveglieri, Z.W. Pan and Z.L. Wang, *Appl. Phys. Lett.* 82 **(2001)** 1869.

[10] Vila, F. Hernandez-Ramırez, J. Rodriguez, O. Casals, A. Romano-Rodrıguez, J.R. Morante and M. Abid, *Mater. Sci. Eng. C* 26 **(2006)** 1063.

[11] F. Hernandez-Ramırez, A.Tarancon,O. Casals, J. Arbiol, A. Romano-Rodrıguez and J.R.Morante*Sensors and Actuators B* 121 **(2007)** 3

[12] J.L. Gole, Z.L. Wang, SnOx nanocrystallites supported by silica nanostructures, *Nano Lett.* 1 **(2001)** 449–451.

[13] Z.R. Dai, Z.W. Pan, Z.L. Wang, Novel nanostructures of functional oxides synthesized by thermal evaporation, *Adv. Funct. Mater.* 13 **(2003)** 9–24.

[14] R.S. Katiyar, P. Dawson, M.M. Hargreave, G.R. Wilkinson, Dynamics of the rutile structure. III. 16. Lattice dynamics, infrared and Raman spectra of SnO2, *J. Phys. C: Solid State Phys.* 4 **(1971)** 2421–2431

[15] S.C. Chang, Oxygen chemisorption on tin oxide: correlation between electrical conductivity and EPR measurements, *J. Vac. Sci. Technol.* 17 **(1980)** 366.

[16] T. Jinkawa, G. Sakai, J. Tamaki, N. Miura, N. Yamazoe, Relationship between ethanol gas sensitivity and surface catalytic property of tin oxide sensors modified with acidic or basic oxides, *J. Mol. Catal. A Chem.* 155 **(2000)** 193–200.

[17] Y. Liu, E. Koep, M. Liu, A highly sensitive and fast-responding $SnO_2$ sensor fabricated by combustion chemical vapor deposition, *Chem. Mater.* 17 **(2005)** 3997–4000.

[18] J.-J. Ho, Y.K. Fang, K.H.Wu,W.T. Hsieh, C.H. Chen, G.S. Chen, M.S. Ju, J.-J. Lin, S.B. Hwang, High sensitivity and ethanol gas sensor integrated with a solid-state